Meteoritics & Planetary Science 38, Nr 6, 831–848 (2003)
Abstract available online at http://meteoritics.org

Transmission electron microscopy of minerals in the martian meteorite Allan Hills 84001

David J. BARBER[1*] and Edward R. D. SCOTT[2]

[1]Physics Centre and Department of Biological Sciences, University of Essex, Colchester CO4 3SQ, UK, and School of Chemical and Life Sciences, University of Greenwich at Medway, Chatham Maritime, ME4 4TB, UK
[2]Hawai'i Institute of Geophysics and Planetology, University of Hawai'i at Manoa, Honolulu, HI 96822, USA
[*]Corresponding author. E-mail: DavidBarber@dbmatcon.demon.co.uk

(Received 28 October 2002; revision accepted 9 June 2003)

Abstract–We have studied carbonate and associated oxides and glasses in a demountable section of Allan Hills 84001 (ALH 84001) using optical, scanning, and transmission electron microscopy (TEM) to elucidate their origins and the shock history of the rock. Massive, fracture-zone, and fracture-filling carbonates in typical locations were characterized by TEM, X-ray microanalysis, and electron diffraction in a comprehensive study that preserved textural and spatial relationships. Orthopyroxene is highly deformed, fractured, partially comminuted, and essentially unrecovered. Lamellae of diaplectic glass and other features indicate shock pressures >30 GPa. Bridging acicular crystals and foamy glass at contacts of orthopyroxene fragments indicate localized melting and vaporization of orthopyroxene. Carbonate crystals are >5 μm in size, untwinned, and very largely exhibit the $R\bar{3}c$ calcite structure. Evidence of plastic deformation is generally found mildly only in fracture-zone and fracture-filling carbonates, even adjacent to highly deformed orthopyroxene, and appears to have been caused by low-stress effects including differential shrinkage. High dislocation densities like those observed in moderately shocked calcite are absent. Carbonate contains impact-derived glasses of plagioclase, silica, and orthopyroxene composition indicating brief localized impact heating. Stringers and lenses of orthopyroxene glass in fracture-filling carbonate imply flow of carbonates and crystallization during an impact. Periclase (MgO) occurs in magnesite as 30–50 nm crystals adjacent to voids and negative crystals and as ~1 μm patches of 3 nm crystals showing weak preferred orientation consistent with $(111)_{MgO}//(0001)_{carb}$, as observed in the thermal decomposition of $CaCO_3$ to CaO. Magnetite crystals that are epitaxially oriented at voids, negative crystals, and microfractures clearly formed in situ. Fully embedded, faceted magnetites are topotactically oriented, in general with $(111)_{mag}//(0001)_{carb}$, so that their oxygen layers are aligned. In optically opaque rims, magnetites are more irregularly shaped and, except for the smallest crystals, poorly aligned. All magnetite and periclase crystals probably formed by exsolution from slightly non-stoichiometric, CO_2-poor carbonate following impact-induced thermal decomposition. Any magnetites that existed in the rock before shock heating could not have preserved evidence for biogenic activity.

INTRODUCTION

The meteorite ALH 84001 is an igneous orthopyroxenite which crystallized on Mars around 4.4 Gyr (Nyquist et al. 2001). It contains about 95% Ca-poor orthopyroxene ($En_{70}Wo_3$), the balance being chromite, maskelynite, and carbonate (~1 vol%) with trace amounts of augite, apatite, olivine, and pyrite (Mittlefehldt 1994; McSween and Treiman 1998). ALH 84001 differs mineralogically from other martian meteorites in 2 major ways: 1) the others contain only trace amounts of carbonate phases; and 2) orthopyroxene (opx) is generally rare, otherwise occurring in Chassigny (McSween and Treiman 1998). The carbonates in ALH 84001 are pre-terrestrial, their compositions being generally less ferroan than those in the nakhlites (Bridges et al. 2001). The meteorite experienced at least one major impact at ~4.0 Gyr (see Nyquist et al. 2001). This age is indistinguishable from the formation age of the carbonates but because of analytical uncertainties, these 2 events might be separated by tens to hundreds of millions of years (Borg et al. 1999). Treiman (1998) inferred that ALH 84001 suffered numerous impacts before and after carbonate formation as well as intense

thermal metamorphism prior to carbonate formation. Greenwood and McSween (2001) argued that carbonate was deposited in the interval between 2 shock events. The origin of the carbonate and associated magnetite remains controversial. This is partly due to the possible presence of fossil relics of martian biogenic processes (McKay et al. 1996; Thomas-Keprta et al. 2000, 2001, 2002) and partly due to major disagreements about the formation temperature of the carbonate (McSween and Treiman 1998).

Despite the considerable interest in the ALH 84001 carbonates and their associated magnetites and sulfides, few published transmission electron microscope (TEM) studies of these phases in situ exist apart from early work by McKay et al. (1996) and Bradley et al. (1996, 1998). Numerous abstracts offer tantalizing glimpses but limited detailed information, e.g., Brearley (1998a, b), Blake et al. (1998), Bell et al. (1999), and Treiman and Keller (2000). We approached the carbonates in ALH 84001 from a perspective gained from TEM studies of many types, including biogenic carbonates (e.g., Wilmot et al. 1992). Textural characteristics can place limits on time-temperature histories, e.g., various types of modulated (Reeder and Wenk 1979; Reeder 1992) and/or dendritic microstructures in carbonates may arise during low temperature growth (Reeder 1992) or by the unmixing of complex compositions (e.g., Barber and Khan 1987). Other clues come from solution-grown carbonates that possess characteristic sector boundaries when formed at low temperature under near equilibrium conditions (Reeder and Prosky 1986; Reeder 1992). We sought microstructural clues (Wenk et al. 1983) that might assist in understanding the origin and history of the carbonates. Difficulties arise mainly from: 1) their unusual compositions (corresponding microstructural data do not exist); 2) the paucity of physico-chemical data on complex carbonates; and 3) the dearth of microstructural observations at the TEM scale on carbonates that have suffered natural or laboratory shock.

Here, we present findings from a comprehensive TEM study designed to preserve textural and spatial relationships between minerals in ALH 84001. The results include deformation effects in opx and carbonate and new observations on the dispositions of magnetite and periclase in carbonate relating to their origins.

Occurrences of Carbonates and Related Minerals

The most spectacular carbonate occurrences in thin sections of ALH 84001 are the 200–500 μm-sized grains, which are associated with plagioclase glass at interstitial sites between the mm- to cm-sized opx crystals. These massive occurrences typically have complex chemical zoning patterns with some regions showing concentric zoning; rounded inclusions of plagioclase glass are common in Mg-poor portions (e.g., Fig. 3c in Shearer et al. [1999]; Fig. 3g in Scott et al. [1998]). Smaller occurrences tend to show a single magnesite zone at one end (e.g., Fig. 1 in Harvey and McSween [1996]). Because rare examples show 2–5 incomplete globules with magnesite-breunnerite rims and siderite-ankerite cores (e.g., Fig. 20 in McSween and Treiman [1998]), massive carbonates have also been called globular carbonates.

Most carbonate grains occur in heavily deformed opx crystals or in fracture zones, apparently occupying what were once fractures and pores (e.g., Fig. 3d in Scott et al. [1998]). However, Treiman (1998) questions whether carbonate formed in void spaces and argues that carbonate replaced plagioclase glass. In fracture zones (also called granular bands or crush zones), carbonate grains enclose opx fragments and extend within and between them (e.g., Figs. 1c in both Treiman [1998] and Scott [1999]). Treiman (1998) refers to these fracture zone carbonates and others that enclose plagioclase glass rather than opx as "framework or poikilitic globules." Warren (1998) calls them "poikilotopic" carbonates. We refer to carbonates in fracture zones and inside heavily deformed opx crystals as fracture-zone and fracture-filling carbonates.

On broken rock surfaces, disk- or pancake-shaped varieties of carbonate, which are not associated with plagioclase glass, may be prominent (e.g., Fig. 2 of McKay et al. [1996]; Scott and Krot 1999). In polished sections, these carbonates typically occur as rods or lenses in resealed fractures, e.g., Fig. 1b in Scott (1999) and Figs. 1c and 1f in Scott et al. (1998). Note that some authors do not distinguish between carbonate globules and disks (e.g., Warren 1998).

The various forms of carbonate in ALH 84001 are chemically zoned and define similar trajectories in Ca-Mg-Fe compositional space, suggesting that they crystallized in similar ways (e.g., Scott et al. 1998). However, Treiman (1998) argues on textural grounds that some carbonates in fractures were melted and mobilized long after the massive carbonates formed at low temperature. Eiler et al. (2002) infer from their geochemical data that ankeritic carbonates formed after magnesio-siderites, and Corrigan and Harvey (2003) suggest that a variety of magnesite associated with Ca-rich carbonate formed after other carbonates.

Proposed Origins for Carbonates

Romanek et al. (1994) and Valley et al. (1997) inferred from isotopic data that the carbonates formed from aqueous fluids at low temperature (<80ºC and <300°C, respectively). Mittlefehldt (1994) favored formation at high temperature (>650ºC), possibly through a reaction between the rock and a CO_2-rich fluid, a view supported by Harvey and McSween (1996). Others have argued that carbonate replaced plagioclase glass (e.g., Treiman 1998). However, minerals that form during dissolution of silicate by CO_2-rich fluids are absent in ALH 84001. Scott et al. (1997, 1998) suggested that carbonate crystallized from shock-induced melts or fluids that

were dispersed into fractured opx during the impact that formed the fracture zones. Many authors argue for precipitation in voids at much lower temperatures. For example, Warren (1998) and Greenwood and McSween (2001) suggest that the carbonates precipitated from evaporating floodwater at ambient temperatures after the creation of fracture zones and before another shock mobilized feldspathic glass. However, Golden et al. (2000, 2001) synthesized amorphous carbonates at 25°C and found that temperatures of 150°C were required to form crystalline zoned carbonates. Eiler et al. (2002) favored aqueous precipitation for all but the ankeritic carbonate: at ~190°C for the sideritic cores and at 200°C for the magnesite rims. The ankeritic carbonate was thought to have formed by shock melting of magnesio-siderites. Vecht and Ireland (2000) inferred from the morphologies described by McKay et al. (1996) that carbonates originally may have formed at low temperature (~25°C) as vaterite (a hexagonal polymorph) and subsequently transformed to calcite. Kirschvink et al. (1997) argued, on the basis of paleomagnetic results, that the carbonates had formed below 110°C, but this was questioned by Scott et al. (1998) and Treiman (1998). Other authors have argued from stable isotope data for formation at low temperature (e.g., Saxton et al. 1998; Warren 1998) or at low or high temperature (Leshin et al. 1998; Treiman and Romanek 1998).

Possible terrestrial analogues, which were formed by hydrothermal and aqueous activity, have been described by Treiman et al. (2002) and Kazmierczak and Kempe (2003).

Magnetite

Magnetite crystals in carbonate have become the focus of debate about evidence for martian life. Thomas-Keprta et al. (2000, 2001) argued that some magnetites are chemically and morphologically indistinguishable from those produced by one strain of magnetotactic bacteria. Chains of magnetites in carbonate have been cited as additional evidence for a bacterial origin (Friedmann et al. 2001). Bradley et al. (1996, 1998) argued, however, that vapor phase growth is responsible for magnetites with elongated forms, citing epitaxy with carbonate and morphological characteristics. Buseck et al. (2001) and Golden et al. (2003) questioned the morphological evidence for a bacterial origin. Two other origins for magnetite have been proposed: precipitates from aqueous solutions (e.g., Blake et al. 1998) and decomposition products of ferroan carbonate following shock heating (Brearley 1998b; Barber and Scott 2002). Thomas-Keprta et al. (2002) criticized the thermal decomposition hypothesis citing the poor correlation between the locations of magnetites and voids and evidence for thermal breakdown of Fe, Mg carbonates to produce Mg-Fe spinels, not pure magnetite (e.g., Chai and Navrotsky 1995). However, Golden et al. (2001) decomposed Fe-rich carbonate to fine-grained magnetite by briefly heating it to 470ºC. Koziol and Brearley (2002) concluded that in oxygen-rich environments, Mg, Fe carbonates decompose to form Mg-rich magnetite, but under oxygen-poor conditions, pure magnetite forms.

SAMPLES AND EXPERIMENTAL PROCEDURE

A doubly-polished thin section (#353), supplied by the NASA Johnson Space Center, was first studied using optical microscopy and Zeiss DSM-962 and Hitachi S-800 field emission scanning electron microscopes (SEMs). Some fusion crust was present, but no work was done on this part of the sample or on adjacent regions that might have suffered thermal alteration. The positions of carbonates and other important features were marked on a grid overlay for correlation with SEM and TEM results. The whole section was mapped by SEM, and particular mineral assemblages were studied using energy-dispersive X-ray analysis (EDX).

Pieces of the demounted section were glued to TEM grids with epoxy resin. To make specimens by beam-milling, we used a modified Ion-Tech (Teddington, U.K.) machine with FAB (fast atom beam) sources, working at 5 kV, with low intensities and low angles of beam incidence to avert the risk of thermal alteration. TEM beam intensities were limited, and electron doses were minimized to avoid radiation damage and thermal alteration of carbonate and sulfide phases. Selected areas were examined with Philips CM20, JEOL 200-CX, and 2010 analytical TEMs, all operated at 200 kV, using TEM imaging, EDX, and electron diffraction. Electron probe sizes were selected (smallest: 1–10 nm in diameter) to give optimum X-ray count rates compatible with the sizes of the chosen crystals and to avoid degradation during microanalysis. Calibration with standards enabled reliable quantitative EDX data to be obtained. A minimum exposure method (Barber et al. 1983) was employed when lattice imaging.

TEM studies were carried out on regions of particular interest that would be accessible and still easily recognizable after beam-milling. This was facilitated by using copper TEM grids (Pelco GC7-Hex™) that could sustain atom bombardment and, subsequently, provide both mechanical support and reference points. The grids were examined by TEM many times, each session being followed by atom-milling of short duration to advance the electron-transparent volumes into pristine new areas.

RESULTS

Our findings bring together optical and electron-optical observations but in illustrating our findings, we have chosen TEM images predominantly because SEM images abound in the literature. TEM-based methods reveal internal features and information that are often lacking with SEM. Unless otherwise stated, we refer to carbonate with >80 mol%

$MgCO_3$ as magnesian carbonate and consider magnesite to be >95 mol% $MgCO_3$. Carbonates with <80 mol% $MgCO_3$ we call ferroan or Fe-rich carbonate. These do not exclude the possibility of ankerite, a term we apply only when electron diffraction patterns contain the extra reflections appropriate to the $R\bar{3}$ (ankerite) structure and that are absent for the $R\bar{3}c$ (calcite) structure.

Orthopyroxene

The opx rock-mass has been strongly deformed and is unrecovered (i.e., minimal subsequent thermal equilibration so that the dislocation substructure is not polygonized). The grains are witness to intense but non-uniform plastic deformation accompanied by variable amounts of microfracturing. Examples of relatively mild deformation effects that have not produced a significant degree of transformation to a different phase are illustrated in Figs. 1a–1c. The deformation seen in these images is consistent with operation of the well-known (100)[001] slip system (Rayleigh et al. 1971; Coe and Müller 1973). High resolution TEM studies also reveal incipient deformation effects. These include multiple microfracturing, which commences on a very fine scale (Fig. 1d) and initiates the conversion of single crystal opx into a polycrystalline aggregate. These features would not be detected by most other techniques, and the defocus method is best for revealing them.

TEM images from opx grains close to and within the fracture zones exhibit evidence of phase alteration due to shock (Fig. 2). It takes several forms: 1) breakdown to fibrous morphologies (sometimes accompanied by bridging needle-like crystals in small vesicles (vugs); 2) more pervasive transformation to clinopyroxene, which occurs as many thin lamellae parallel to (100) planes; 3) formation of sheets and wide lamellae of shock-formed glass of opx composition (opx glass), ~3–100 nm wide (glass of this composition was reported by Bell et al. [1999]); and 4) frothy glass at fracture intersections. Shock formation of fibrous morphologies of opx and bridging needle-like crystals in vugs (Fig. 2a) have not been reported previously. The needles are not a hydrous silicate to judge by the lattice spacings derived from their diffraction patterns, although we note that Barker and Banfield (1999) reported very minor amounts of smectite at the carbonate-pyroxene interface, which were inferred to be

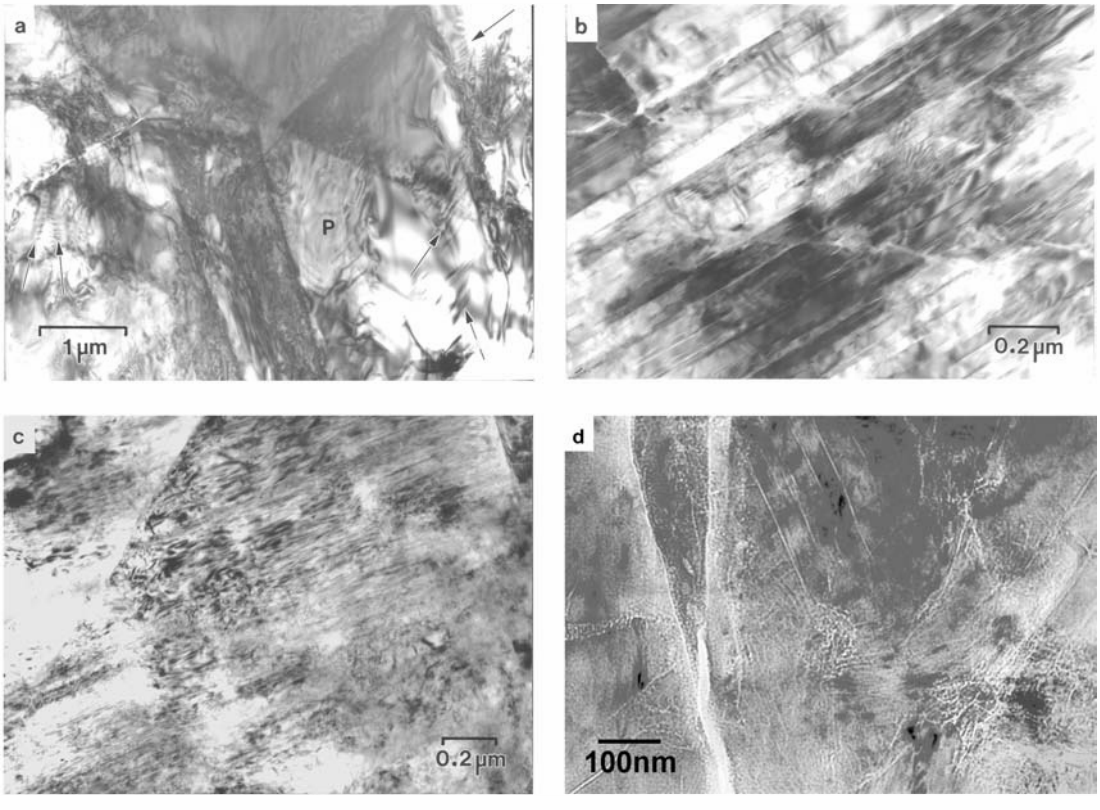

Fig. 1. TEM images showing typical deformation effects in grains of orthopyroxene from near a fracture zone: a) heterogeneous deformation and fracturing producing lattice strain and dislocations (the latter are visible where arrowed and in the region labelled [P]); the dark regions are caused by strong diffraction contrast where there are concentrations of dislocations and some microfracturing; b) deformation on separated slip planes producing some stacking faults, which are thin (100) lamellae of clinopyroxene representing partial transformation (see Ashworth and Barber 1976); c) profuse deformation by (100)[001] slip; d) incipient shock-induced alteration in the form of fine-scale cataclasis and loss of single-crystal character; the effects have been enhanced by applying a small amount of defocus.

terrestrial in origin. The fibrous opx appears to form by microfracturing on parallel (001) planes producing strips of silicate that can kink. Small microvesicles generated by the deformation are bridged by needle-like crystals, which we postulate are the result of redeposition from hot silicate vapor.

Figures 2b and 2c illustrate the stronger shock-induced alteration effects, classified above as (3) and (4). The creation of thin parallel (100) lamellae due to the ortho- to clino- inversion during deformation is well documented, occurring under both low stress and shock conditions (Coe and Müller 1973; Kirby and Coe 1974; Ashworth and Barber 1976). The presence of glass cross-cutting the intergrowth of ortho and clinopyroxene lamellae generates a blocky microstructure (Fig. 2b) and indicates that shock pressures of 30–40 GPa were attained locally (Leroux 2001). The cross-cutting glassy sheets are not strictly planar when seen at TEM magnifications, but if thicker versions were seen optically, they would probably be classified as planar deformation features (PDFs). (Optically visible planar defects were reported by Scott et al. [1998].) The pyroxene blocks (Fig. 2b) are commonly separated by very thin lamellae of glass parallel to (100) planes and at most a few interplanar spacings in thickness, which might be called nanoscale PDFs. Frothy opx glass (Fig. 2c) is another feature that does not appear to have been reported previously, but frothy glass is well-known in other shocked silicates where it

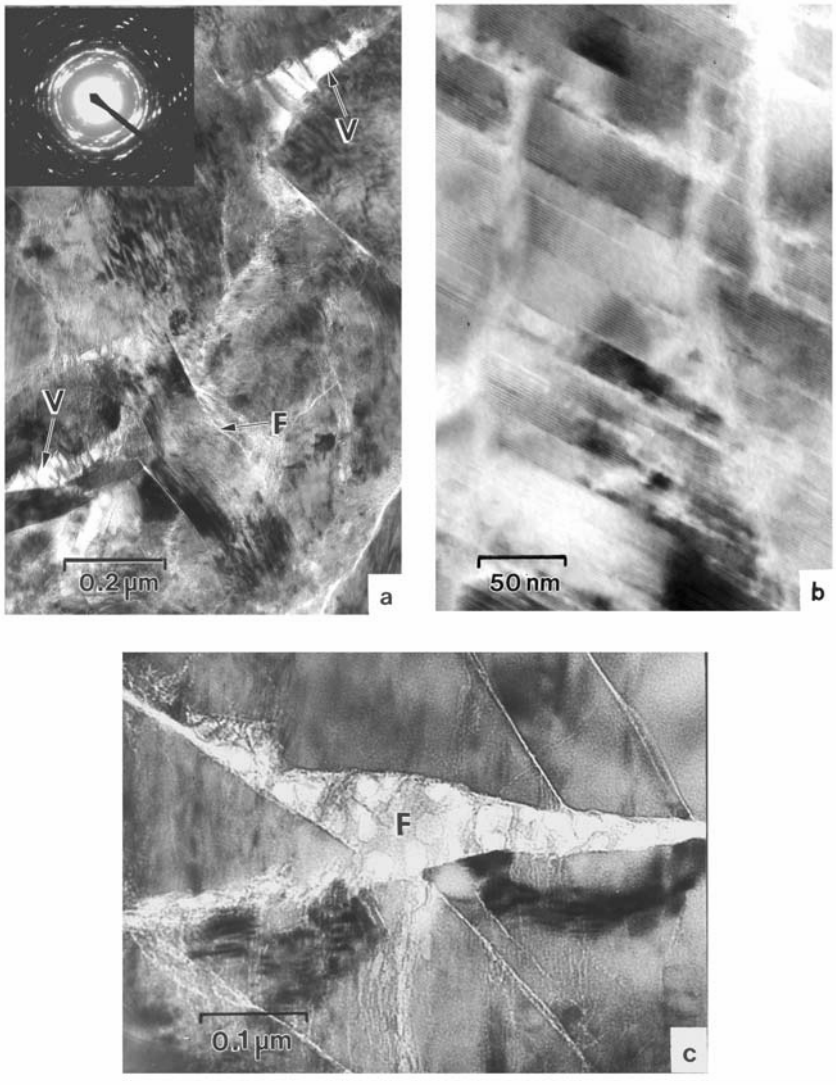

Fig. 2. TEM images showing examples of stronger shock-induced alteration in orthopyroxene (opx): a) strong shock deformation producing curved fibrous morphologies (e.g. [F]) and small vesicles (V) with bridging acicular crystals. The inset shows a selected area diffraction pattern with asterism demonstrating the polycrystallinity produced; b)shock-induced, cross-cutting sheets of opx glass (nearly vertical light bands), which produce a blocky structure of mixed ortho- and clino-lamellae; glassy lamellae also occur on (100) planes and have widths of a few interplanar spacings; c) frothy opx glass (F) filling intersecting microfractures in orthopyroxene. Note that some fragment edges appear to be corroded. The vesicular microstructure of the melted and solidified glassy opx in the microfracture is characteristic of shock-melted minerals.

is indicative of moderate-to-high peak shock pressures (e.g., Kieffer et al. 1976).

Finally, we note 2 examples where there appears to be a connection between the shock deformation in opx and the nature of the adjacent carbonate. At the boundary between opx and some fracture-filling carbonates, we found stringers of opx glass lining the interface (Fig. 3a). Within the carbonate, stringers of opx glass are oriented parallel to the opx/carbonate interface and lens-like glass inclusions also exist. The second example in Fig. 3b shows another interface between opx and magnesian carbonate that is inclined to the electron beam. Large bubble-like voids lie on the interface; smaller voids with various shapes occur nearby in the carbonate.

Carbonates

Deformation Effects

Our section contained 2 adjacent examples of massive carbonate at the edge. The largest, some 200 × 130 μm^2 in area, was located next to a grain of plagioclase glass with carbonate that formed irregular veins and fingers intruding into plagioclase glass and fractures in the adjoining opx. A nearby smaller mass of carbonate contained a partial, curving piece of magnesite rim. This assemblage, shown in Fig. 3c, was the only clear example of a globular carbonate in our section. Carbonate discs did not occur in the section, but fracture-zone and fracture-filling carbonates were abundant.

Before making our TEM observations, we were concerned that some veining apparent in SEM images of the massive carbonate might be a sign of weathering. TEM imaging removed this worry, revealing that the "veining" corresponded to concentrations of porosity, which are widespread in the ALH 84001 carbonates and seem to have a thermal origin. Our reflected light studies of carbonates and those in transmitted light of globules by M. S. Bell (personal communication, 2001) suggest that carbonate crystal sizes are 50–100 μm and that globules and disks are typically single or double crystals. TEM is not a good method for assessing grain

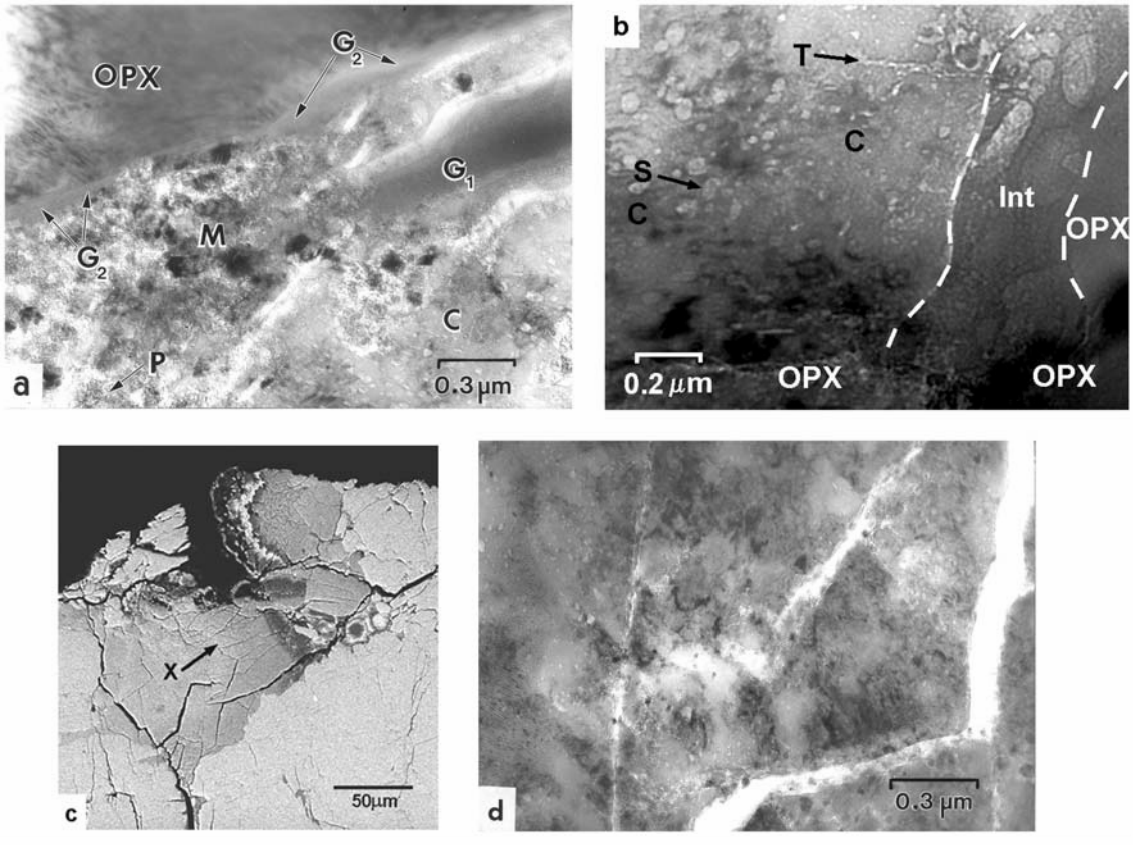

Fig. 3. a) TEM image of a stringer of opx glass (G1) within carbonate, which fills a mainly μm-wide fracture in orthopyroxene. Another thinner stringer of opx glass (arrows, G2) separates the opx grain from the carbonate. The carbonate (C) has many faceted voids; around M, it appears to have decomposed to magnetite (dark crystals), together with much fine-grained periclase, e.g., at (P); b) TEM image of a region containing an inclined contact surface between magnesian carbonate (C) and orthopyroxene (OPX), with large bubble-like voids on the interface (labelled [Int] and defined by broken white lines) and smaller more euhedral voids (e.g., [S]) and tubes (T) within the carbonate; c) 15 kV SEM image showing massive (globular) carbonate at the edge of the thin section, with a piece of magnesian rim; d) TEM image from the region marked (X) in Fig. 3c, showing undeformed carbonate but with "old" cleavage cracks and transverse fractures, which are regions where magnetite crystals (small, mostly dark features) and euhedral voids seem to be mainly concentrated.

size because of the small areas that are thin at any one time. However, our results confirm that crystals in the massive carbonate, including the magnesian rim, are >5 µm in size; certainly not submicrometer in size, as is sometimes inferred (e.g., Kazmierczak and Kempe 2003). Except for carbonates of ankeritic composition that give diffraction patterns indicating crystallization with the $R\bar{3}$ dolomite structure, magnesian and Fe-rich carbonates exhibit the $R\bar{3}c$ calcite structure. A few instances of what we believe are fine-scale intergrowths of the $R\bar{3}c$ and $R\bar{3}$ structures were noted in interstitial carbonates.

Neither the massive ferroan carbonate nor the adjacent magnesian rim showed any clear evidence for deformation when imaged using TEM. Figure 3d is an image of massive ferroan carbonate at the region marked (X) in Fig. 3c. It shows cleavage cracks and fractures, but dislocations or other signs of plastic deformation are absent. Negative crystals and magnetites were present, both being distributed heterogeneously. In general, massive carbonate lacked subgrain boundaries and individual dislocations, but cleavage cracks and transverse fractures frequently caused minor misorientations that were mainly responsible for asterism in the corresponding diffraction patterns. In the ferroan carbonate, these cracks were seldom "clean" and often contained fine-grained materials, magnetite being the most easily recognizable.

Despite the general absence of deformation, some fracture-zone and fracture-filling carbonates appear to have suffered local mild plastic deformation (e.g., see Figs. 4a and 4c), which gives rise to varying degrees of asterism in the diffraction patterns, e.g., Fig. 4b. In fracture-filling carbonates, we found inclusions of plagioclase glass and stringers or lenses of opx glass (Fig. 3a). Some veins of plagioclase glass appeared to have formed by the intrusion of plagioclase melt into carbonate (Fig. 4d). The carbonate adjacent to the glass contains many voids and abundant magnetite, but such features also often occur where no glass is present.

Oxides and Voids

Many carbonate regions, unlike those in Figs. 4a and 4c, show inclusions of magnetite (Fe_3O_4) and periclase (MgO) together with voids. In Barber and Scott (2002) we focused on features of the oxides and voids that we interpreted as evidence for shock-induced thermal decomposition of

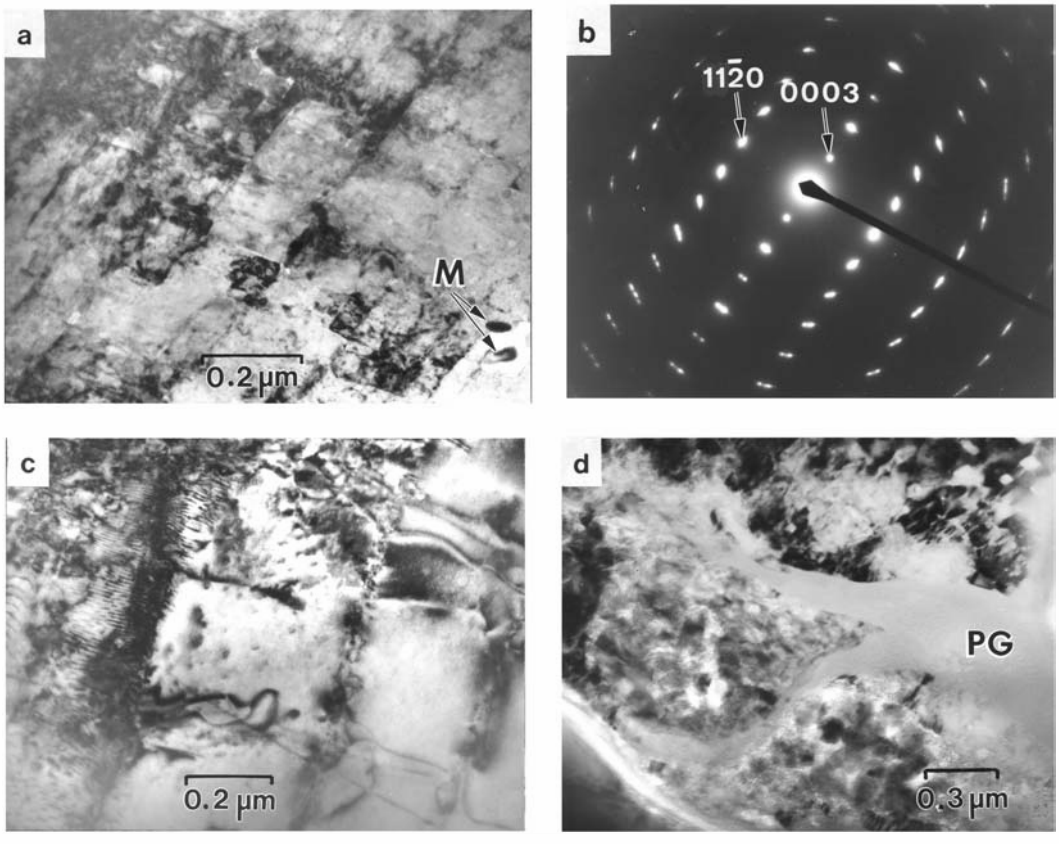

Fig. 4. TEM images illustrating mild deformational and other effects in fracture-filling ferroan carbonate: a) blocky microstructure created in ankerite by displacements on 2 different sets of crystallographic {10$\bar{1}$4} planes, with some fine cleavage fractures; b) electron diffraction pattern from the blocky ankerite imaged in (a) showing asterism due to misorientations between the small blocks; c) slip bands and some linking dislocations; d) tongues of plagioclase glass (PG) intruding into carbonate, probably by local melting along fractures. The carbonate contains both voids and irregularly-shaped magnetite crystals.

carbonate and loss of CO_2. Here, we present additional evidence that bears on the origin of the oxides and voids.

Both rim- and fracture-filling magnesian carbonate contain MgO, which occurs as ~1 μm-sized patches of polycrystalline nm-sized oxide, sometimes with a weak texture (Fig. 1a in Barber and Scott [2002]). Diffraction rings from the MgO are weak and somewhat diffuse. MgO occurs in both magnesian and ferroan carbonate but in the latter it is difficult to identify by diffraction in the presence of magnetite (the 200 and 220 rings for MgO occur at almost the same radii as the 400 and 440 rings for Fe_3O_4). In magnesian regions of massive carbonate, the patches of MgO occur adjacent to "old" fractures and open porosity. MgO also occurs as individual crystals, (typically 30–50 nm in diameter) either within or growing into tiny voids in the carbonate (Fig. 1c in Barber and Scott [2002]). The characteristic microstructure of nano-scale, periclase-carbonate intergrowths (e.g., Fig. 1a of Barber and Scott [2002]) usually allows MgO to be recognized even when associated with Fe_3O_4 in ferroan carbonate (Figs. 5a–5c).

Massive magnesian carbonate also contains small voids. These are generally rounded or irregular in form, unlike the majority of voids in the Fe-rich carbonates, which are commonly euhedral. (This may reflect the more demanding

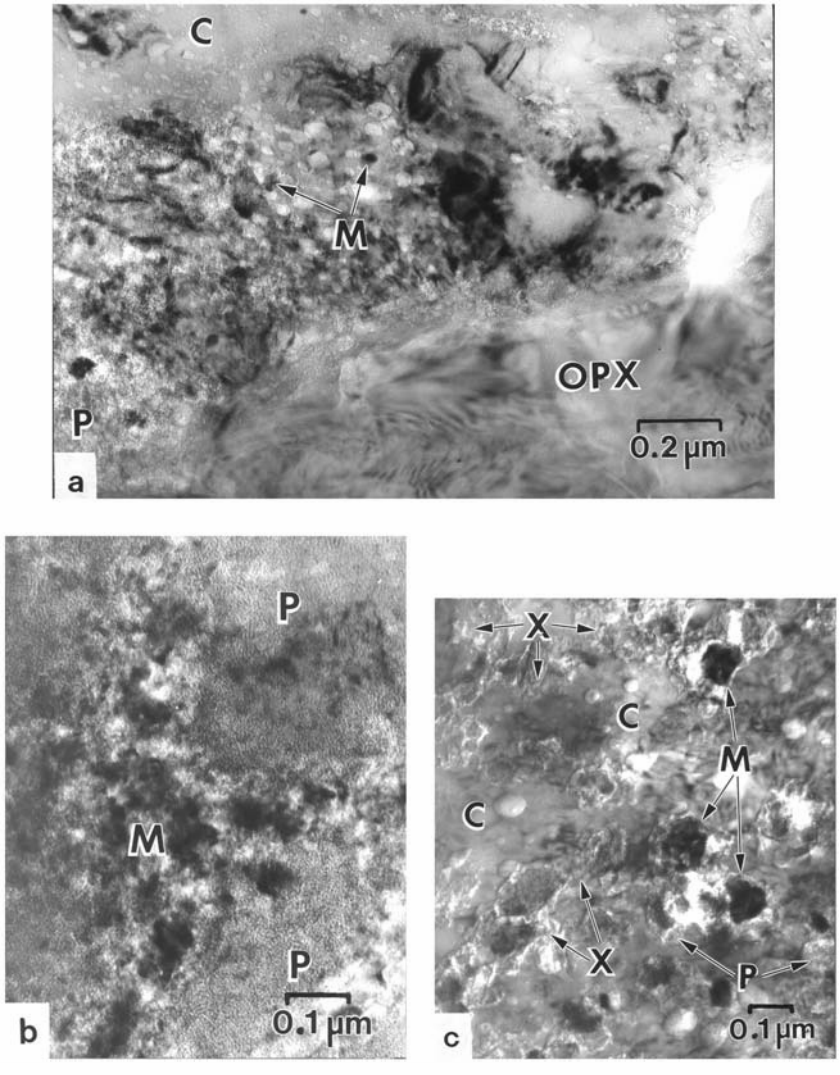

Fig. 5. TEM images illustrating close spatial relationship between magnetite (M) and periclase (P) in ferroan carbonate (C): a) direct contact between heavily shocked orthopyroxene (OPX) and carbonate (C), showing that the void size and concentration of oxides tends to vary with increasing distance from the heavily shocked pyroxene. Magnetites (M) and some small patches of periclase (P) are present and intimately intermixed; b) image showing larger patches of nanocrystalline periclase (P) together with irregularly-shaped magnetite crystals (M) in ferroan carbonate. The diffraction contrast at the upper (P) comes from some residual carbonate within or underlying the patch of periclase; c) magnetite crystals (e.g., [M]), carbonate (e.g., at [C]) and MgO nanocrystalline material (e.g., [P]). The granular material in the small regions typified by those labelled X appear to be polyphasic and some lime may be present. We cannot exclude the possibility that some redeposition of carbonate has occurred in the voids where materials with unusual morphologies are visible.

time/temperature conditions needed to equilibrate magnesite, which is more refractory than the mixed carbonate.) Voids in the magnesite are usually empty, but a small proportion contain a tiny crystal (see Barber and Scott 2002). The fractures in the magnesite are not clean but are partially filled with material that exhibits either incipient or fully developed decomposition effects; they appear to be "old." The finding that magnesite has partially decarbonated to yield MgO led us to think that the crystallites seen in a few of the rounded voids are also MgO, an idea which is supported by EDX data.

Magnetite crystals have various forms and sites in ferroan carbonate and ankerite (Barber and Scott 2002). Figure 6a shows elongate forms of Fe_3O_4 (called whiskers by some authors) protruding from the carbonate into a large microfracture and also growing within the solid. Figures 6b and 6c show magnetite within "old" fractures and within opx, respectively. Magnetites in magnetite-rich rims on massive carbonate and in analogous locations in fracture-filling and fracture-zone carbonate are usually variable in size and shape, e.g., Fig. 7a, and they are mostly larger than the more isolated individuals. The ring diffraction patterns from rim magnetite sometimes show a preferred orientation, as in Fig. 7b. (Topotactic relationships between carbonate and individual magnetites that are fully embedded have already been reported [Barber and Scott 2002].) Ferroan carbonate frequently possesses zones with high concentrations of small voids, as in the magnesian variety. Therefore, such zones of high porosity appear to be widespread in all the carbonates but especially seem to occur close to changes in composition (e.g., near magnetite-rich rims) and close to fracture surfaces and other interfaces.

Where numerous voids and high oxide concentrations occur, Fe_3O_4 and fine-grained MgO are both found. Patches of MgO (with a low Fe-content) also tend to exhibit weak preferential orientations, e.g., Fig. 5b. This is consistent with the finding of Kim et al. (1987) that $MgCO_3$ decomposes topotactically to a porous MgO product, which pseudomorphs the original carbonate. Now that we have identified both iron oxide and magnesium oxide, we anticipate that a small amount of lime, CaO, may also be present (because of the Ca, Mg, Fe content of the carbonate), but this is difficult to prove.

We explored the structural condition of the carbonate matrix towards the periphery of a magnetite-rich rim, where magnetite particles are still mostly separate, using selected area diffraction and combined bright- and dark-field images (Figs. 7c and 7d). The continuity of the carbonate lattice is maintained as indicated by the selected area diffraction pattern of Fig. 7b, which shows a single reciprocal lattice pattern from carbonate superposed on a ring pattern from magnetite. We do not find carbonate to have a small grain size, as reported by Thomas-Keprta et al. (2000), but rather a substructure of small subgrains, typically 20–150 nm in diameter. These findings are confirmed by the matched bright field and dark field images of Figs. 7c and d.

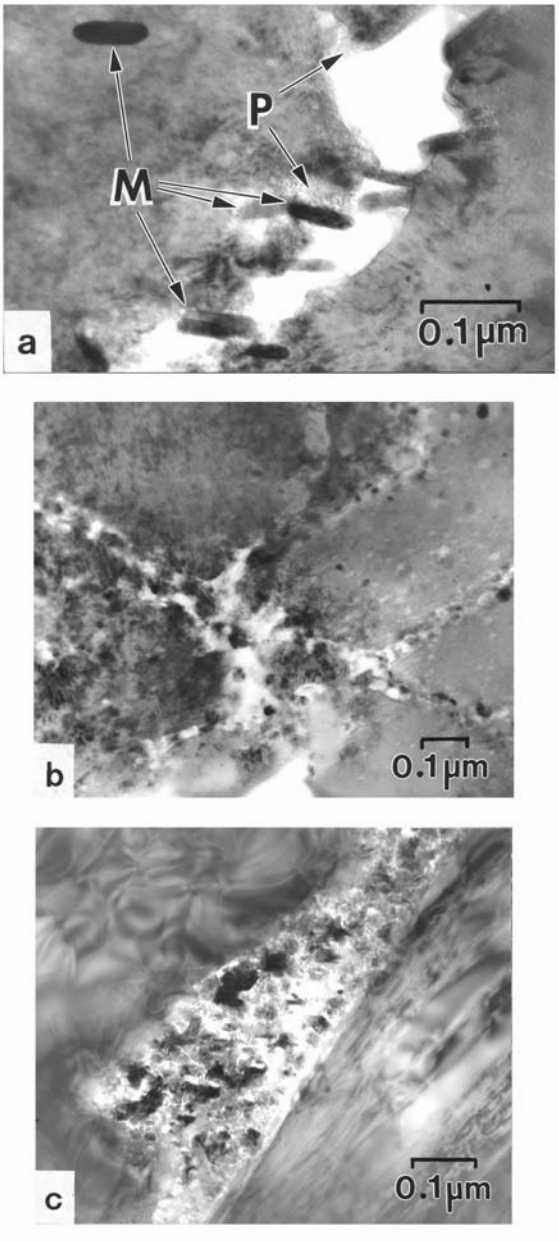

Fig. 6. TEM images of magnetite in void spaces in carbonate and orthopyroxene: a) elongate crystals of magnetite (arrows, M) growing into a microfracture in massive ferroan carbonate and similar individual in the solid. The arrows (P) point to tiny patches of MgO; b) magnetite crystals (probably with minor amounts of periclase) concentrated on fracture surfaces in deformed fracture-filling ankerite; c) abundant magnetite crystals with minor carbonate in an interstice in a fracture-zone orthopyroxene crystal. This magnetite occurrence resembles the finer-grained part of opaque rims of massive carbonates.

In summary, the oxides observed in massive, fracture-filling, and crush zone carbonates appear to be rather similar in their morphologies, distributions, and dispositions in voids and within carbonate. Currently, we are less certain about the compositions of the magnetite and periclase and whether

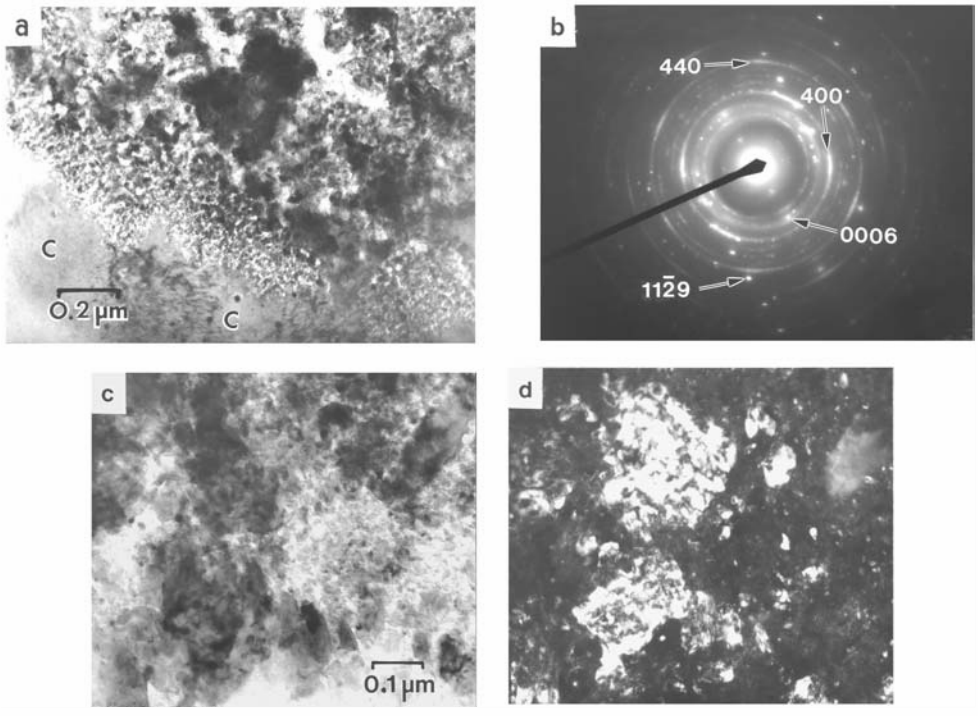

Fig. 7. TEM images from materials in a magnetite-rich rim: a) interface between ferroan carbonate (C) and magnetite-rich rim, showing irregular magnetites with regions of carbonate existing within the magnetite; b) diffraction pattern from a ~2 μm^2 area within a magnetite-rich rim showing a single carbonate reciprocal lattice pattern superimposed on a ring pattern from magnetite; c) and d) matching bright field and dark field images from the carbonate in the magnetite-rich rim showing the subgrain structure. Even though continuity of the carbonate lattice is almost destroyed, regions ~200 nm across are very closely related in orientation and diffract similarly as shown by (d), indicating that they are really subgrains of a much larger crystal. Numerous small magnetites are also "lit" by the 11$\bar{2}$0 reflection used to create image (d), showing that they are specially oriented with respect to the carbonate lattice.

these vary with location, i.e., we do not know whether MgO embedded in ferroan carbonate contains FeO, and we do not have good limits on the amount of MgO in Fe_3O_4.

DISCUSSION

Orthopyroxene and Shock History of ALH 84001

The highly deformed, fractured and partially comminuted, (Figs. 1a–1c) and essentially unrecovered nature of the deformed opx, with the characteristics of the fracture zones that we have encountered, are testament to the violent shock history of ALH 84001. These shock effects account for the optical properties of the opx noted by Scott et al. (1998). The images in Fig. 1 show opx that has been strongly deformed and/or fractured but shows only slight evidence of transformation. The images of Fig. 2 illustrate regions of stronger deformation that have led to significant amounts of phase transformation (to glass or clinopyroxene) or to another type of alteration. Although some differences in detail exist because of the heterogeneity of the minerals in ordinary chondrites, the behavior of ALH 84001 opx is comparable to that found in shock-stage S4–6 ordinary chondrites and similarly shocked meteorites (e.g., Ashworth and Barber 1975; Ashworth 1985). As is commonly the case for S4–6 chondrites, multiple shock events for ALH 84001 (e.g., Treiman 1998) cannot be excluded but are not required to account for the pyroxene microstructures.

Grains of plagioclase glass and rarer silica glass found by Scott et al (1997) indicate formation from a melt and not through solid-state processes. However, the relative scarcity of glassy silicates and the absence of large vesicles of the type formed in them by shock pressures ~50 GPa suggests that the maximum shock pressures experienced were somewhat lower than that value. Raman spectroscopy of interstitial grains has shown that some plagioclase melted at temperatures >1200ºC (Cooney et al. 1999), suggesting shock pressures >35 GPa (Stöffler et al. 1991; Yamaguchi and Sekine 2000). The alteration of monocrystalline opx to give fibrous microstructures, microvesicles, and bridging acicular crystals are interesting new effects which are also attributable to shock. The needle-like crystals probably form by the deposition of volatilized silicate. Ashworth (1985) noted that partial melting of silicate minerals was implied by the formation of microvesicles. He interpreted thin veins of glass in pyroxenes as evidence of vapor deposition rather than solid-state phase transformation (although the direct formation of glass lamellae by shock deformation is well

known in quartz). The transformation to diaplectic glass and the generation of small amounts of foamy glass at grain fragment-to-fragment contacts in ALH 84001 point to significant shock pressures. The transformation of opx to form diaplectic glass lamellae with "blocky" remanent crystals (Fig. 2b) and the generation of small volumes of foamy opx glass at fracture intersections (Fig. 2c) also indicate peak shock pressures >30 GPa.

According to Stöffler et al. (1991), the presence of opx glass indicates high local shock pressures (as high as 80 GPa). However, we know that TEM often exposes effects that are overlooked with other lower resolution techniques (e.g. Figs. 2b and 2c). Thus, TEM can lead to the overestimation of shock pressures if applied to features that were calibrated with optical microscopy (e.g., Schmitt 2000). The stringers of opx glass that line the boundaries between opx and some fracture-filling carbonates (Fig. 3a) may have formed as a result of frictional heating due to shear stresses at the shock edges, as in shock-induced pseudotachylites (Kenkman et al. 2000).

Oxides in Carbonate

Our discovery of periclase in magnesian carbonate and topotactically oriented magnetite in ferroan carbonate provide powerful evidence that these oxides formed by solid-state exsolution following decarbonation (Barber and Scott 2002). The intimate association of the carbonate with shock-formed plagioclase and opx glass provides strong evidence for shock-induced decomposition of carbonates to their oxides, which curiously has not yet been observed in terrestrial impact craters (Osinski and Spray 2001). Evidence for the formation of magnetite in ALH 84001 by thermal decomposition of ferroan carbonate was provided by Golden et al. (2001). The association between voids and magnetite crystals was previously discussed by Brearley (1998b) and Scott et al. (1997) and attributed to decomposition of Fe-rich carbonate to magnetite during shock heating. We infer, however, that the formation of magnetite on fracture surfaces, within negative crystals (and within the solid for the smallest population of magnetite crystals) are manifestations of cooling a slightly non-stoichiometric oxide-rich carbonate (effectively CO_2-poor) that, thus, became supersaturated. Diffusion of point defects, such as carbonate ion vacancies, interstitial cations, and oxygen ions (e.g., Fisler et al. 2000) allowed voids and magnetite crystals to form at separate locations.

We believe that both periclase and magnetite formed by exsolution from the solid state, which favors the nucleation of tiny single crystals and a tendency for them to have crystallographic relationships to the host carbonate. Magnetites linked to tiny voids and negative crystals and also magnetites fully embedded in carbonate are products of exsolution in our view. The epitaxial nature of members of the first 2 types has been demonstrated by Bradley et al. (1998) and Blake et al. (1998). Magnetites that are surrounded by carbonate are topotactically oriented, mainly with $\{111\}_{mag}//(0001)_{carb}$ and $\{110\}_{mag}//\{11\bar{2}0\}_{carb}$), as reported for the decomposition of calcite into lime (McTigue and Wenk 1985), showing that magnetite nucleated and grew in situ (Barber and Scott 2002). We use the term "topotaxy" advisedly. It derives from Lotgering (1959) who applied it to "all chemical solid state reactions that lead to a material with crystal orientations which are correlated with crystal orientations in the initial product." Topotaxy between magnetites and carbonate is characteristic of a solid state reaction such as dehydration, decarbonation, or exsolution (i.e., precipitation in the solid state).

We view the species, sizes, and locations of oxide crystals in carbonate to be primarily functions of the Fe/Mg ratio, local variations in diffusivity and availability of nuclei due to the presence of internal surfaces (e.g., microfractures), vacancies, voids, and other defects. The amounts of oxides formed would have been affected by local variations in shock heating because voids can concentrate at carbonate contacts with opx, e.g., Fig. 5a, or glass. Magnetite formation tends to correlate with high concentrations of porosity but also occurs on open internal surfaces. The lesser extent of decomposition of magnesian carbonate, in general, compared with the breakdown of the more ferroan carbonates, is consistent with experimental studies (e.g., Chang et al. 1998). Exsolution of epitaxial magnetite in faceted voids ~50 nm across (negative crystals) is common and both features indicate that all species of vacancies and Fe ions were mobile. At the rims of carbonate crystals, where magnetites and voids are more abundant, the Fe-rich carbonate has broken down more completely to give agglomerates of magnetite particles, which have strained the carbonate and produced a microstructure of small (~200 nm) subgrains. Magnetites in the rims tend to be more irregular in size and shape, and epitaxy with the decomposing host lattice is less favored (because they are formed under far-from-equilibrium conditions) than when they nucleate and grow separately.

The gradual decomposition of calcite, aragonite, dolomite, and magnesite-rich carbonates produces crystals and needles of oxides that correspond to the original cation contents (McTigue and Wenk 1985; Burrage and Pitkethly 1969; Cater and Buseck 1985; Kim et al. 1987; Reeder 1992). Under favorable conditions, the oxide crystals are epitaxial with the remaining carbonate, but a porous mass of oxide results from further decomposition. The formation of Fe_3O_4 on fracture surfaces, in negative crystals and within solid carbonate, therefore, indicates different conditions from simple decomposition, as these locations are, in descending order, the energetically preferred sites for nucleation and growth from unstable solute-rich solid solutions. Although the MgO patches observed bear similarities to oxides formed as simple decarbonation products, the characteristics and dispositions of individual oxide crystals lead us to envisage a more complex scenario of exsolution from cooling unstable,

non-stoichiometric carbonates containing excess oxides that resulted from shock-heating. Post-shock temperatures were high enough to allow limited diffusion and equilibration to occur after decarbonation so that exsolution is to be expected.

Analogous morphological behavior is found in systems where solute precipitation is used for decoration of dislocations, e.g., Ag and Au in alkali halides (Amelinckx 1956; Barber et al. 1957). In these systems, metallic precipitates form when cooling the host crystal from a temperature where the halide compound (AgCl and $HAuCl_4$, respectively) is in solution. In diffusion-doped sodium chloride, euhedral-shaped crystals of gold form epitaxially within small negative crystals as illustrated in Fig. 8 (Harvey 1960), which should be compared to Figs. 1c and 1e of Barber and Scott (2002). Such negative crystals form on cooling melt-grown sodium chloride that is probably slightly chlorine deficient. Smaller gold crystals generally precipitate on any dislocations present and also often within the solid at distances greater than the diffusion length from defects. The dark appearance of the cavity walls in Fig. 8 is due to Fresnel fringes generated from the out-of-focus parts of the walls; no evidence of exists finer-scale precipitation on the walls. The close parallels between the behaviors of the alkali halide and carbonate systems strengthen our conviction that the Fe_3O_4 and MgO nanocrystals exsolved from carbonate.

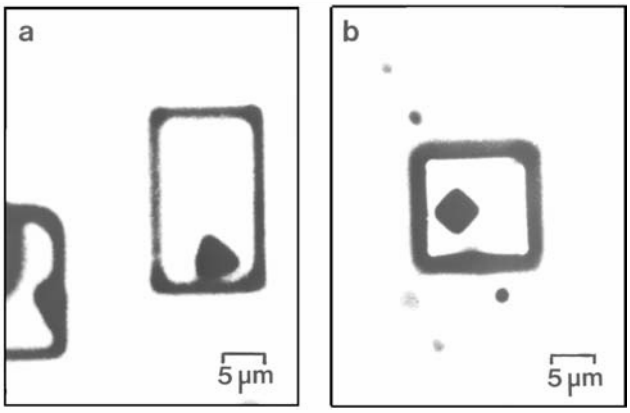

Fig. 8. Optical images showing solid state exsolution of gold crystals from doped sodium chloride (from Harvey 1960). Each of the euhedral voids (negative crystals) contains an euhedral gold crystal that grew epitaxially when a melt-grown, doped sodium chloride crystal, which was probably slightly chlorine deficient, was cooled. Similarities between the occurrences of magnetite and periclase in voids in ALH 84001 carbonate (Figs. 1c and 1d in Barber and Scott [2002]) support formation of the martian oxides by exsolution during cooling.

Supposedly Biogenic Magnetite

Thomas-Keprta et al. (2000, 2001) examined ~600 magnetite crystals that were acid-extracted from ALH 84001 carbonate and concluded that ~28% were truncated hexa-octahedral crystals (formerly called elongated prismatic by Thomas-Keprta et al. [2000]) of biogenic origin. Their conclusion was based on the similarity in crystal size, shape, and composition to the magnetites produced by one strain of magnetotactic bacteria and the presence of features in the carbonate resembling chains of magnetosomes (Friedmann et al. 2001). The other magnetite crystals that were acid-extracted by Thomas-Keprta et al. (2000) were found to be highly elongated crystals with width/length ratios <0.4 (7%) or irregularly shaped (65%).

Thomas-Keprta et al. (2000) argued that the supposedly biogenic forms were located mainly in the magnetite-rich rim carbonate and that epitaxial magnetites, which are clearly abiogenic, were located elsewhere, citing the small grain size of the carbonate in the rim (stated to be as small as 10 nm). To the contrary, we find that rim carbonate is neither fine-grained nor lacks long-range order, as claimed, but rather that it is highly strained by the presence of a large volume-fraction of magnetite, imparting a subgrain microstructure. Rim magnetite consists mostly of irregularly-shaped crystals and appears to represent the uncontrolled decomposition of particularly Fe-rich carbonate. Thus, the general lack of epitaxy or topotaxy of magnetite with carbonate in rims is not surprising. Although epitaxy is a sign of abiotic crystal growth, its absence does not imply biogenesis. We are convinced that the population of euhedral-shaped magnetites largely occurs as individual crystals in the carbonate rather than in the rim-like material. While the population includes the rare whisker-like types that are undoubtedly abiogenic (Bradley et al. 1998), Thomas-Keprta et al. (2001) identified mostly more-equiaxed faceted crystals with morphologies like the truncated hexa-octahedral type.

The topotactic orientation of the fairly equiaxed faceted magnetite crystals provides strong evidence that they formed in the carbonate and could not have been formed elsewhere by bacteria. Magnetites in magnetotactic bacteria are synthesized with a high degree of mutual alignment in order to endow the cell with a net magnetic dipole. This is induced because the magnetic nanocrystals adopt particular growth planes and crystal habits in the parent cell, facilitating the alignment of the orientations and easy directions of magnetization (e.g., Mann and Frankel 1989). Thus, magnetotactic bacteria carefully align the magnetites within the cell but cannot align them with extracellular carbonate crystal. Once the cell tissue holding the magnetite crystals in place has been destroyed, the special orientation of the magnetites will be lost so that they cannot be precisely aligned inside a carbonate crystal. The chain-like arrangements of magnetites that characterize magnetotactic bacteria would also be destroyed, as noted by Thomas-Keprta et al. (2002). Epitaxial growth of a carbonate crystal on a magnetosome might permit one oriented magnetite in a carbonate crystal to be biogenic but not the thousands that are present within each carbonate crystal in ALH 84001.

If magnetites were present in carbonate before the shock heating event that heated the carbonate, they could not have

survived intact. Even supposing that such magnetites were completely impervious to the shock wave and immune to any reaction with the shock-heated (or shock-melted) carbonate, they would certainly have acted as nucleation sites during subsequent cooling. Thus, any magnetites in carbonate before impact heating would have been coated with new layers of magnetite up to tens of nanometers in thickness. Martian organisms cannot, therefore, be responsible for the size and shape of any magnetite crystal in carbonate.

Some chain-like groups of magnetites in ALH 84001 have been attributed to their having bacterial origins (Friedmann et al. 2001), but such linear dispositions are also consistent with abiotic mechanisms. In this context, other workers have cited alignment in magnetic fields, formation in narrow channels, etc. However, a very common reason for linear arrangements seems to have been overlooked, namely, the low-energy nucleation sites provided on crystal surfaces by atomic-scale terraces and ledges, which are proven by calculation (e.g., see Tiller 1991) and demonstrable by several methods of surface physics. Under near-equilibrium conditions, nucleation at kink sites and ledges on surfaces is favored over nucleation at defects, like dislocations, or solute clustering on lattice sites. Such heterogeneous nucleation is well-known and can account for chains of crystals. The general lack of dislocations in the ALH 84001 carbonates makes the decoration of dislocations an unlikely explanation for chains of magnetites.

Thomas-Keprta et al. (2000, 2002) argue that 6 specific properties of certain magnetite crystals in ALH 84001 and MV1 bacteria should constitute a biosignature or "magnetic assay for biogenicity." However, plausible reasons exist to explain why some magnetites that form by thermal decomposition of iron-bearing carbonate should mimic the biogenic crystals. For example, a tendency for magnetites that precipitate topotactically in carbonate to be elongated along [111] may result from the preference for this direction be aligned parallel to the unique 3-fold rotation axis in the carbonate structure. Elongation along [111] naturally promotes the development on the predominantly octahedral forms of 6 of the {110} faces that are in the [111] zone. Thus, single-domain magnetites with truncated hexa-octahedral shapes should not be considered as a definitive biosignature. If one accepts the claims that biogenic magnetites with these properties occur in ALH 84001, one must ask where they are located, why demonstrably abiogenic magnetites should have such similar properties, and how biogenic and abiogenic crystals could have been intimately mixed and oriented in carbonate.

We did not study magnetites in disk-shaped carbonates, which form in fractures, but the magnetites in these carbonates are probably very similar to those in the massive and fracture-filling carbonates. Bradley et al. (1998) studied carbonate from a fracture surface, which was probably disk-shaped, and our TEM observations on magnetite are consistent with theirs. The massive carbonate that we studied is clearly similar to the globular carbonate studied by McKay et al. (1996), and SEM and electron-probe studies suggest that carbonate globules and disks have similar properties. These carbonates all show the same Fe-Mg-Ca zoning and have magnetite-rich zones next to magnesite, typically at the periphery of the grain. Thomas-Keprta et al. (2000) obtained their magnetites by acid dissolution, but carbonate is the only mineral in ALH 84001 that is soluble in acetic acid. We, therefore, conclude that the magnetites that we studied are entirely representative of those that were dissolved out by Thomas-Keprta et al. (2000).

Carbonates

We found no support for the idea that the ALH 84001 carbonates formed by replacement of plagioclase glass (e.g., Treiman 1998). Plagioclase glass is intimately mixed with some carbonates but no replacement textures were observed. Formation of carbonate in voids is much more plausible. Two different models have been proposed (Warren 1998, 1999; Scott and Krot 1999; Scott 1999). In both models, carbonate formed at low temperatures from CO_2-rich aqueous or hydrothermal fluids (e.g., Bridges et al. 2001) and partly decomposed to oxides during a brief heating event (Golden et al. 2001; Barber and Scott 2002).

The carbonate microstructures seen by TEM differ considerably from those known for low temperature terrestrial carbonates or from aqueously formed calcite and Mn-dolomite in CM2 chondrites (Barber 1981; Grady et al. 1987). Electron-optical fringes that could be attributed to finescale compositional heterogeneities (e.g., intergrowths of the $R\bar{3}c$ and $R\bar{3}$ structures) in the ankeritic and ferroan carbonates are rarely seen. Such effects are common in many terrestrial low temperature carbonates (Reeder 1992). Aqueously-grown calcites and dolomites are usually poorly crystalline and defect laden, in strong contrast to the highly crystalline ALH carbonates. The absence of typical features such as modulated microstructures and growth sector boundaries (Reeder 1992) indicates formation temperatures well above 100°C. However, for these features, we cannot exclude growth at low temperatures followed by some very localized equilibration that preserved the micron-scale Mg-Fe-Ca zoning. Golden et al. (2000) also favor temperatures above 100°C, as the carbonates they grew at 25°C were amorphous and chemically distinct from those in ALH 84001. However, the carbonates that Golden et al. grew at 150°C have a radiating growth texture of needle-shaped crystals (Fig. 8d of Golden et al. [2000]) that is absent in the ALH carbonates, contrary to what Treiman (2001) and others have stated. The absence of this radiating growth texture in ALH carbonates cannot, as Golden et al. imply, be attributed to overprinting by impact deformation effects, as these are mild. Nor is it possible that such textures were completely removed

by solid-state recrystallization. If the carbonate crystals, which are many micrometers in width, had grown by grain boundary migration in the solid, their μm-scale chemical zoning would have been erased by diffusion.

Only mild deformation effects were observed in the fracture-zone and fracture-filling carbonates (Fig. 4), with even weaker effects in the massive carbonate (Fig. 3d), implying that the deformation in the fracture zone and fracture-filling carbonates was of variable and low intensity. Carbonate crystallized after the impact or impacts that created the fracture zones and probably after the cross-cutting glassy veins and localized melts in opx were formed (Fig. 2). Slip-generated, high dislocation densities, which occur in moderately shocked calcite (Barber and Wenk 1979), are absent. Cleavage and fracture, which are more prevalent than slip, seem to indicate deformation at low-to-moderate temperature (<400ºC), but some of the cracking probably arose from differential cooling effects. Some cleavages have healed and oxides have exsolved, so at this stage of the carbonate's history, some recovery was possible. Differential shrinkage on cooling and other low stress effects mostly post-date the last thermal event, which was probably the shock that caused decarbonation and triggered exsolution of magnetite. Putting certain limits on the time and temperature conditions is difficult because the properties of magnesite/siderite solid solutions are not known. Lack of twinning in the carbonates is consistent with the properties of the observed magnesitic and sideritic compositions and, thus, does not help to constrain conditions. On the basis of what is known about calcite and dolomite (e.g., Wenk et al. 1983), we deduce that the post-deformation temperature was below 500ºC within a few minutes of the event.

The microstructure of bubbles and tubes adjacent to the opx surface in Fig. 3b suggests that the carbonate was briefly very hot. If the carbonates crystallized before the impact that heated them and not during this event, the energy for heating the carbonate must have been deposited by the shock and associated frictional deformation outside the carbonate. The idea that impact-formed hot plagioclase glass or melt was responsible for heating carbonates and causing their decomposition has been discussed by Brearley (1998a). Although this is possible, e.g., Fig. 4d, we doubt that it was a major heating mechanism because much carbonate is not associated with plagioclase glass and no correlation exists between the abundance of oxides and vugs in carbonate and the local concentration of plagioclase glass.

The shapes and distribution of the stringers or lenses of opx glass at the boundary between carbonate and opx and within the carbonate (e.g., Fig. 3a) suggest that the glass solidified while the carbonate was fluid. The high aspect ratios of their shapes are not compatible with an origin as eroded glass fragments. Therefore, the glass stringers do not appear to be simply fragments of glass from the opx boundary or glass that was injected after the carbonate formed. The orientations of the stringers follow the periphery of the opx grain, not a carbonate fracture plane, suggesting that carbonate flowed. These features favor carbonate crystallization during an impact event.

Unfortunately, shock experiments do not illuminate the history of the ALH 84001 carbonates because the conditions under which carbonates melt or decompose are not well constrained. In addition, TEM has scarcely been used in studies of experimentally-shocked carbonates. Many studies suggest that calcite and dolomite remain crystalline up to shock pressures ~60 GPa, but the onset of significant decarbonation and development of pores probably occurs at less than half this value (e.g., Lange and Ahrens 1986). Calcite also becomes highly porous at pressures approaching 50 GPa with the formation of vesicles in the sub-mm range. Such vesicles are absent in the ALH 84001 carbonates, although much smaller voids are abundant. At lower shock pressures, the heating is less homogeneous and is concentrated at cleavage surfaces, where loss of CO_2 will, therefore, be most severe initially. This conforms with our observation of lacy regions adjacent to fractures and zones where voids are concentrated. Shock experiments by Agrinier et al. (2001) show that decarbonation can be followed by growth of secondary carbonate. We found no evidence for the latter and infer that much of the released CO_2 escaped through fractures. Few shock experiments appear to have melted carbonates, though recent studies of terrestrial impact structures indicate that carbonates can be mobilized as melts during impacts (Graup 1999; Osinski and Spray 2001). Discrepancies between laboratory shock results on carbonate and differences from natural impact products have been attributed to variations in ambient CO_2 pressures, the extent of localized shear bands, porosity, shock duration, grain size, mineralogy, etc. (e.g., Agrinier et al. 2001).

Our studies of fracture-filling and massive carbonates, together with most published studies of their chemical and isotopic zoning (Treiman 1998), generally suggest that all carbonates in ALH 84001 crystallized in the same process. However, Eiler et al. (2002) argue that Ca-rich and Ca-poor carbonates have different histories. Differences exist in the deformation experienced by different types of carbonates as noted above, and compositional variations may also exist. Three of the carbonate grains that we selected to show deformation effects are ankerite (Figs. 4a, 4b, and 6b). The apparent predominance of deformation effects in ankerite could have several causes: 1) fractures and dislocations may form more readily in ankerite than in the Mg- and Fe-rich carbonates; 2) Ca-rich carbonate crystallized before other varieties and may, therefore, have experienced more deformation; and 3) ankerites have a different origin. The first explanation is doubtful, although the ease of deformation twinning, for example, does depend on carbonate composition. More data are needed to test the other 2 explanations. Our observations seem to counter the idea of

Eiler et al. (2002) that ankeritic carbonates formed by shock melting of the magnesian and ferroan carbonates (which would favor the ankerites being the least deformed).

The deformational and other microstructural features do not reveal how the ALH 84001 carbonates formed. They probably experienced transient temperatures well above 1000°C because the fracture-zone and fracture-filling carbonates are intimately associated with plagioclase and opx glasses. The mild deformation in all carbonates suggests that they crystallized after the opx was strongly deformed to create glass and the fracture zones were introduced. Such features are easier to understand if carbonate crystallized during an impact event that made monomineralic glasses and partly decomposed carbonate to oxides. If all carbonates crystallized by the same process, the massive carbonates also crystallized in this impact.

Sulfide in Carbonate

Sulfide is intimately mixed with magnetite in the Fe-rich rims of carbonate globules (McKay et al. 1996), but its nature and origin remains uncertain. McKay et al. (1996) reported 2 sulfides in a carbonate globule. In the Fe-rich rim, they found ~5 vol% pyrrhotite in the form of euhedral crystals up to 100 nm across and rounded 20–60 nm polycrystalline particles. In the carbonate core, they reported 100 nm long Fe-sulfides, which did not diffract, appeared to be unstable in the electron beam, and were thought to be greigite. Bradley et al. (1998) questioned the identification by McKay et al. (1996) of both sulfides and suggested that the sulfides might be polymorphs of pyrrhotite or "unit cell-scale intergrowths of sulfides and magnetite, perhaps resulting from the partial oxidation of sulfides." By contrast, Weiss et al. (2002) found abundant pyrrhotite mixed with magnetite in a carbonate rim.

Like Bradley et al. (1998), we could not identify any sulfide phase in our section with certainty, besides pyrite (Mittlefehldt 1994), even when there was a strong EDX signal for sulfur. A few additional faint diffraction rings were occasionally seen, but rings from phases other than magnetite were usually absent. The sulfur may occur mostly as very fine-grained iron sulfide or possibly as an amorphous phase, perhaps as a coating on the magnetite grains. No evidence was found for the formation of magnetite from sulfide.

Since sulfides occur in opx fractures, as in shocked ordinary chondrites (e.g., Scott et al. 1998), sulfide was likely mobilized during shock heating as Foley et al. (1998) inferred. They found sulfide blebs on cleavages within S-rich carbonate disks and suggested that sulfide was emplaced by shock after carbonate crystallized. Some of this sulfide may have precipitated from carbonate. Clearly, the presence of sulfide in the carbonate, even closely associated with magnetite, does not require that some magnetite is detrital, as McKay et al. (1996) argued.

Magnetization of ALH 84001

The origins of magnetite and carbonate in ALH 84001 have considerable bearing on the natural remanent magnetization (NRM) of the rock, as this is largely carried by the magnetite, which is mainly single domain (Weiss et al. 2000, 2002; Antretter et al. 2003). Kirschvink et al. (1997) inferred from the heterogeneous magnetization of opx crystals that they were rotated during the formation of the fracture zones and that the rock was not subsequently heated above 110°C. Since the carbonates formed after the fracture zones, they inferred that the carbonates formed below 110°C. This is incompatible with our TEM evidence for exsolution of magnetite and equilibrated euhedral voids, which require the diffusion of point defects including solute atoms over distances of a few hundred nanometres. Kent et al. (2001) show that bulk diffusion over these distances is insignificant in Ca-rich carbonates below 200ºC and in Mg-rich carbonates below 400ºC.

Weiss et al. (2000) proposed that the heterogeneous magnetization of opx was due to localized shock heating that selectively remagnetized the rock. Our studies suggest an alternative explanation. Given that most magnetites are single-domain and elongated along [111] (Thomas-Keprta et al. 2000), and this direction is generally parallel to the trigonal axis of the carbonate crystal as we infer, the apparent direction of magnetization of each carbonate crystal will tend to be aligned along the trigonal axis of each carbonate crystal. Then, opx crystals that contain only a few carbonate crystals would tend to be magnetized at diverse angles when exposed to the same field.

Since the magnetite formed in a major impact heating event and the last major impact heating event occurred at 4.0 Gyr when Ar was lost (see Nyquist et al. 2001), it is probable that the magnetite and the rock magnetization date from this time. The field intensity then was an order of magnitude smaller than the current terrestrial field (Antretter et al. 2003; Weiss et al. 2002).

The origin of the ALH 84001 magnetite may also bear on the origin of the martian magnetic anomalies. The inferred crustal magnetization is an order of magnitude larger than that typically found in earth rocks (Stevenson 2001) and probably results from abundant single-domain magnetite crystals (Kletetschka et al. 2000). Our study suggests one mechanism for forming such magnetite in the martian crust.

CONCLUSIONS

Our results are strong evidence that the condition of the carbonates, together with the disposition of the magnetite and periclase, are indirect witnesses to the shock history of ALH 84001. The decomposition of carbonates by shock-heating has generated both magnetite and periclase, an idea that we advanced previously (Barber and Scott 2002) and which is

supported by the work of Brearley (1998b). We believe that the vast majority and probably all of the magnetite grains have a physico-chemical origin. Any magnetites existing in the rock before shock heating could not have preserved evidence for biogenic activity. We conclude that the carbonate crystallized in the presence of hot, impact-formed silicate melts and that fracture-filling and fracture-zone carbonates subsequently suffered mild deformation due to post-shock grain displacements and differential cooling stresses. We propose that carbonates, oxides, and sulfides with biogenic origins have yet to be identified in ALH 84001.

Acknowledgments–We thank the NASA Johnson Space Center Curatorial Facility for the sample; W. Barker, V. Stähle, and A. Treiman for helpful reviews; and many colleagues for helpful discussions. We also thank the Librarian of the University of Bristol, U.K. for permission to reproduce figures from the Ph.D. thesis of Harvey (1960). This work was partially supported by NASA grant 5–4212 (K. Keil) and National Science Foundation grant number OPP-9714012 (E. Scott). This is Hawai'i Institute of Geophysics and Planetology Publication No. 1291 and School of Ocean and Earth Science and Technology Publication No. 6180.

Editorial Handling—Dr. Allan Treiman

REFERENCES

Agrinier P., Deutsch A., Schärer U., and Martinez I. 2001. Fast back-reactions of shock-released CO_2 from carbonates: An experimental approach. *Geochimica et Cosmochimica Acta* 65: 2615–2632.

Amelinckx S. 1956. In *Dislocations and mechanical properties of crystals,* edited by Fisher J. C., Johnston W. G., Thomson R., and Vreeland T. New York: John Wiley & Sons.

Antretter M., Fuller M., Scott E., Jackson M., Moskowitz B., and Solheid P. Forthcoming. Paleomagnetic record of martian meteorite ALH 84001. *Journal of Geophysical Research.*

Ashworth J. R. 1985. Transmission electron microscopy of L group chondrites, 1. Natural shock effects. *Earth and Planetary Science Letters* 73:17–32.

Ashworth J. R. and Barber D. J. 1975. Electron petrography of shock effects in a gas-rich enstatite-achondrite. *Contributions in Mineralogy and Petrology* 49:149–162.

Ashworth J. R. and Barber D. J. 1976. Shock effects in meteoritic pyroxene. In *Developments in electron microscopy and analysis,* edited by Venables J. A. London: Academic Press. pp. 517–520.

Barber D. J. 1981. Matrix phyllosilicates and associated minerals in C2M carbonaceous chondrites. *Geochimica et Cosmochimica Acta* 45:945–961.

Barber D. J. and Khan M. R. 1987. Composition-induced microstructures in rhombohedral carbonates. *Mineralogical Magazine* 51:71–86.

Barber D. J. and Scott E. R. D. 2002. Origin of supposedly biogenic magnetite in the martian meteorite Allan Hills 84001. *Proceedings of the National Academy of Sciences* 99:6556–6561.

Barber D. J. and Wenk H. R. 1979. On the geological aspects of calcite microstructure. *Tectonophysics* 54:45–60.

Barber D. J., Harvey K. B., and Mitchell J. W. 1957. A new method of decorating dislocations in crystals of alkali halides. *Philosophical Magazine* 2:704–707.

Barber D. J., Freeman L. A., and Smith D. J. 1983. Analysis of high voltage, high resolution images of lattice defects in experimentally-deformed dolomite. *Physics and Chemistry of Minerals* 9:102–108.

Barker W. W. and Banfield J. F. 1999. HRTEM evidence for low temperature alteration of pyroxene to smectite in ALH 84001 (abstract). *Geological Society of Amercia Abstracts with Programs* 31:A432.

Bell M. S., Thomas-Keprta K. L., Wentworth S. J., and McKay D. S. 1999. Microanalysis of pyroxene glass in ALH 84001 (abstract #1951). 30th Lunar and Planetary Science Conference. CD-ROM.

Blake D., Treiman A., Cady S., Nelson C., and Krishnan K. 1998. Characterization of magnetite within carbonate in ALH 84001 (abstract #1347). 29th Lunar and Planetary Science Conference. CD-ROM.

Borg L. E., Connelly J. N., Nyquist L. E., Shih C. Y., Weissman H., and Reese Y. 1999. The age of the carbonates in martian meteorite ALH 84001. *Science* 286:90–94.

Bradley J. P., Harvey R. P., and McSween H. Y., Jr. 1996. Magnetite whiskers and platelets in the ALH 84001 martian meteorite: Evidence of vapor phase growth. *Geochimica et Cosmochimica Acta* 60:5149–5155.

Bradley J. P., McSween H. Y., Jr., and Harvey R. P. 1998. Epitaxial growth of nanophase magnetite in martian meteorite ALH 84001: Implications for biogenic mineralization. *Meteoritics & Planetary Science* 33:765–773.

Brearley A. J. 1998a. Microstructures of feldspathic glass in ALH 840001 and evidence of post carbonate formation shock melting (abstract #1452). 29th Lunar and Planetary Science Conference. CD-ROM.

Brearley A. J. 1998b. Magnetite in ALH 84001: Product of the decomposition of ferroan carbonate (abstract #1452). 29th Lunar and Planetary Science Conference. CD-ROM.

Bridges J. D., Catling D. C., Saxton J. M., Swindle T. D., Lyon I. C., and Grady M. M. 2001. Alteration assemblages in martian meteorites: Implications for near-surface processes. Space *Science Reviews* 96:365–392.

Burrage B. J. and Pitkethly D. R. 1969. Aragonite transformations observed in the electron microscope. *Physica Status Solidi* 32: 399–405.

Buseck P. R., Dunin-Borkowski R. E., Devouard B., Frankel R. B., McCartney M. R., Midgley P. A., Posfai M., and Weyland M. 2001. Magnetite morphology and life on Mars. *Proceedings of the National Academy of Sciences* 98:13490–13495.

Cater E. D. and Buseck P. R. 1985. Mechanism of decomposition of dolomite, $Ca_{0.5}Mg_{0.5}CO_3$ in the electron microscope. *Ultramicroscopy* 18:241–252.

Chai L. and Navrotsky A. 1996. Synthesis, characterization, and enthalpy of mixing of the (Fe, Mg)CO_3 solid solution. *Geochimica et Cosmochimica Acta* 60:4377–4384.

Chang L. L. Y., Howie R. A., and Zussman J. 1998. *Rock-forming minerals, Volume 5: Non-silicates: Sulphates, carbonates, phosphates, halides*. 2nd edition. London: Geological Society of London.

Coe R. S. and Müller W. F. 1973. Crystallographic orientation of clinoenstatite produced by deformation of orthoenstatite. *Science* 180:64–66.

Cooney T. F., Scott E. R. D., Krot A. N., Sharma S. K., and Yamaguchi A. 1999. Vibrational spectroscopic study of minerals in the martian meteorite ALH 84001. *American Mineralogist* 84: 1569–1576.

Corrigan C. M. and Harvey R. P. 2003. Evidence for a second generation of magnesite in martian meteorite Allan Hills 84001 (abstract #1255). 34th Lunar and Planetary Science Conference. CD-ROM.

Eiler J. M., Valley J. W., Graham C. M., and Fournelle J. 2002. Two populations of carbonate in ALH 84001: Geochemical evidence for discrimination and genesis. *Geochimica et Cosmochimica Acta* 66:1285–1303.

Fisler D. K., Gale J. D., and Cygan R. D. 2000. A shell model for the simulation of rhomgohedral carbonate minerals and their point defects. *American Mineralogist* 85:217–224.

Foley C. N., Humayan H., Davis A. M., and Kagan O. 1998. Chemical and SEM studies of mineral assemblages within ALH 84001 (abstract #1928). 29th Lunar and Planetary Science Conference. CD-ROM.

Friedmann I. E., Wierzchos J., Ascaso C., and Winklhofer M. 2001. Chains of magnetite crystals in the meteorite ALH 84001: Evidence of biological origin. *Proceedings of the National Academy of Sciences* 98:2176–2181.

Golden D. C., Ming D. W., Schwandt C. S., Morris R. V., Yang S. V., and Lofgren G. E. 2000. An experimental study on kinetically-driven precipitation of calcium-magnesium-iron carbonates from solution: Implications for the low temperature formation of carbonates in martian meteorite Allan Hills 84001. *Meteoritics & Planetary Science* 35:457–465.

Golden D. C., Ming D. W., Schwandt C. S., Lauer H. V., Socki R. A., Morris R. V., Lofgren G. E., and McKay G. A. 2001. A simple inorganic process for formation of carbonates, magnetite, and sulfides in martian meteorite ALH 84001. *American Mineralogist* 86:370–375.

Golden D. C., Ming D. W., Morris R. V., Brearley A. J., Lauer H. V., Jr., Treiman A., Zolensky M. E., Schwandt C. S., Lofgren G. E., and McKay G. A. 2003. Morphological evidence for an exclusively inorganic origin for magnetite in martian meteorite ALH 84001 (abstract #1970). 34th Lunar and Planetary Science Conference. CD-ROM.

Grady M. M., Graham A. L., Barber D. J., Aylmer D., Kurat G., Ntaflos T., Ott U., Palme H., and Spettel B. 1987. Yamato-82042: An unusual carbonaceous chondrite with CM affinities. *Proceedings of the 11th Symposium on Antarctic Meteorites*. pp. 162–178.

Graup G. 1999. Carbonate-silicate liquid immiscibility upon impact melting: Ries Crater, Germany. *Meteoritics & Planetary Science* 34:425–438.

Greenwood J. P. and McSween H. Y., Jr. 2001. Petrogenesis of Allan Hills 84001: Constraints from impact-melted feldspathic and silica glasses. *Meteoritics & Planetary Science* 36:43–61.

Harvey K. B. 1960. Dislocations, foreign ions, and vacancies in sodium chloride single crystals. Ph. D. thesis, University of Bristol, U.K.

Harvey R. P. and McSween H. Y., Jr. 1996. A possible high-temperature origin for the carbonates in the martian meteorite ALH 84001. *Nature* 382:49–51.

Kazmierczak J. and Kempe S. 2003. Modern terrestrial analogues for the carbonate globules in martian meteorite ALH 84001. *Naturwissenschaften* 90:167–172.

Kenkman T., Hornemann U., and Stöffler D. 2000. Experimental generation of shock-induced pseudotacholites along lithological interfaces. *Meteoritics & Planetary Science* 35:1275–1290.

Kent A. J. R., Hutcheon I. D., Ryerson F. J., and Phinney D. L. 2001. The temperature of formation of carbonate in martian meteorite: Constraints from cation diffusion. *Geochimica et Cosmochimica Acta* 65:311–321.

Kieffer S. W., Phakey P. P., and Christie J. M. 1976. Shock processes in porous quartzite: Transmission electron microscope observations and theory. *Contributions in Mineralogy and Petrology* 59:41–93.

Kim M. G., Dahmen H., and Searcy A. W. 1987. Structural transformation in the decomposition of $Mg(OH)_2$ and $MgCO_3$. *Journal of the American Ceramic Society* 70:146–154.

Kirby S. H. and Coe R. S. 1974. The role of crystal defects in the enstatite inversion. *Transactions of the American Geophysical Union* 55:419.

Kirschvink J. L., Maine A. T., and Vali H. 1997. Paleomagnetic evidence of a low-temperature origin of carbonate in the martian meteorite ALH 84001. *Science* 275:1629–1638.

Kletetschka G., Wasilewski P. J., and Taylor P. T. 2000. Mineralogy of the sources for magnetic anomalies on Mars. *Meteoritics & Planetary Science* 35:895–899.

Koziol A. and Brearley A. 2002. A non-biological origin for the nanophase magnetite grains in ALH 84001: Experimental results (abstract #1672). 33rd Lunar and Planetary Science Conference. CD-ROM.

Lange M. A., and Ahrens T. J. 1986. Shock-induced CO_2 loss from $CaCO_3$; Implications for early planetary atmospheres. *Earth and Planetary Science Letters* 77:409–418.

Leroux H. 2001. Microstructural shock signatures of major minerals in meteorites. *European Journal of Mineralogy* 13:253–272.

Leshin L. A., McKeegan K. D., Carpenter P. K., and Harvey R. H. 1998. Oxygen isotopic constraints on the genesis of carbonates from martian meteorite ALH 84001. *Geochimica et Cosmochimica Acta* 62:3–13.

Lotgering K. F. 1959. Topotactic reactions with ferromagnetic oxides having hexagonal crystal structure, I. *Journal of Inorganic Nuclear Chemistry* 9:113–123.

Mann S. and Frankel R. B. 1989. Magnetite biomineralization in unicellular microorganisms. In *Biomineralization: Chemical and biochemical perspectives,* edited by Mann S., Webb J., and Williams R. J. P. Weinheim: VCH Verlagsgesellschaft. pp. 389–426.

McKay D. S., Gibson E. K., Jr., Thomas-Keprta K. L., Vali H., Romanek C. S., Clemett S. J., Chiller X. D. F., Maechling C. R., and Zare R. N. 1996. Search for past life on Mars: Possible biogenic activity in martian meteorite ALH 84001. *Science* 273: 924–930.

McSween H. Y., Jr. and Treiman A. H. 1998. Martian meteorites. In *Planetary materials,* edited by Papike J. J. Washington D.C.: Mineralogical Society of America. *Reviews in Mineralogy* 36.

McTigue J. W. and Wenk H. R. 1985. Microstructures and orientation relationships in the dry-state aragonite-calcite and calcite-lime phase transformations. *American Mineralogist* 70: 1253–1261.

Mittlefehldt D. W. 1994. ALH 84001, A cumulate orthopyroxenite member of the martian meteorite clan. *Meteoritics* 29:214–221.

Nyquist L. E., Bogard D. D., Shih C. Y., Greshake A., Stöffler D., and Eugster O. 2001. Ages and geologic histories of martian meteorites. *Space Science Reviews* 96:105–164.

Osinski G. R. and Spray J. G. 2001. Impact-generated carbonate melts: Evidence from the Haughton structure, Canada. *Earth and Planetary Science Letters* 194:17–29.

Rayleigh C. B., Kirby S. H., Carter N. L., Ave Lallement H. G. 1971. Slip and the clinoenstatite transformation as competing rate processes in enstatite. *Journal of Geophysical Research* 76: 4011–4022.

Reeder R. J. 1992. Carbonates: Growth and alteration microstructures. In *Minerals and reactions at the atomic scale: TEM,* edited by Buseck P. R. Washington D.C.: Mineralogical Society of America. pp. 381–424. *Reviews in Mineralogy* 27:381–424.

Reeder R. J. and Prosky J. L. 1986. Compositional sector zoning in dolomite. *Journal of Sedimentary Petrology* 56:237–247.

Reeder R. J. and Wenk H. R. 1979. Microstructures in low temperature dolomites. *Geophysical Research Letters* 6:77–80.

Romanek C. S., Grady M. M., Wright I. P., Mittlefehldt D. W., Soicki R. A., Pillinger C. T., and Gibson E. K., Jr. 1994. Record of fluid-rock interactions on Mars from the meteorite ALH 84001. *Nature* 372:655–657.

Saxton J. M., Lyon I. C. and Turner G. 1998. Correlated chemical and isotopic zoning in carbonates in the martian meteorite ALH 84001. *Earth and Planetary Science Letters* 160:811–822.

Schmitt R. T. 2000. Shock experiments with the H6 chondrite Kernouvé: Pressure calibration of microscopic shock effects. *Meteoritics & Planetary Science* 35:545–560.

Scott E. R. D. 1999. Origin of carbonate-magnetite-sulfide assemblages in martian meteorite ALH 84001. *Journal of Geophysical Research* 104:3803–3814.

Scott E. R. D. and Krot A. N. 1999. Comment on "Petrologic evidence for low-temperature, possibly flood-evaporitic origin of carbonates in the ALH 84001 meteorite" by Paul H. Warren. *Journal of Geophysical Research* 104:24211–24215.

Scott E. R. D., Yamaguchi A., and Krot A. N. 1997. Petrological evidence for shock melting of carbonates in the martian meteorite ALH 84001. *Nature* 387:377–9.

Scott E. R. D., Krot A. N., and Yamaguchi A. 1998. Carbonate in fractures of martian meteorite Allan Hills 84001: Petrologic evidence for impact origin. *Meteoritics & Planetary Science* 33: 709–719.

Shearer C. K., Leshin L. A., and Adcock C. T. 1999. Olivine in martian meteorite Allan Hills 84001: Evidence for a high-temperature origin and implications for signs of life. *Meteoritics & Planetary Science* 34:331–339.

Stevenson D. J. 2001. Mars' core and magnetism. *Nature* 412:214–219.

Stöffler D., Keil K., and Scott E. R. D. 1991. Shock metamorphism of ordinary chondrites. *Geochimica et Cosmochimica Acta* 55: 3845–3867.

Thomas-Keprta K. L., Bazylinski D. A., Kirschvink J. L., Clement S. J., McKay D. S., Wentworth S. J., Vali H., Gibson E. K., Jr., and Romanek C. S. 2000. Elongated prismatic magnetite crystals in ALH 84001 carbonate globules: Potential martian magnetofossils. *Geochimica et Cosmochimica Acta* 64:4049–4081.

Thomas-Keprta K. L., Clement S. J., Bazylinski D. A., Kirschvink J. L., McKay D. S., Wentworth S. J., Vali H., Gibson E. K., Jr., McKay M. F., and Romanek C. S. 2001. Truncated hexa-octahedral magnetite crystals in ALH 84001: Presumptive biosignatures. *Proceedings of the National Academy of Sciences* 98:2164–2169.

Thomas-Keprta K. L., Clemett S. J, Bazylinski D. A., Kirschvink J. L., McKay D. S., Wentworth S. J., Vali H., Gibson E. K., Jr., and Romanek C. S. 2002b. *Applied and Environmental Microbiology* 68:3663–3672.

Tiller W. A. 1991. *The science of crystallization: Microscopic interfacial phenomena.* Cambridge: Cambridge University Press.

Treiman A. H. 1995. A petrographic history of martain meteorite ALH 84001: Two shocks and an ancient age. *Meteoritics* 30:294–302.

Treiman A. H. 1998. The history of Allan Hills 84001 revised: Multiple shock events. *Meteoritics & Planetary Science* 33:753–764.

Treiman A. H. 2001. A hypothesis for the abiotic & non-martian origins of putative signs of ancient martian life in ALH 84001 (abstract #1304). 32nd Lunar and Planetary Science Conference. CD-ROM.

Treiman A. H. and Keller L. P. 2000. Magnetite-bearing layers in Allan Hills 84001 carbonate globules: Bulk and mineral compositions (abstract). *Meteoritics & Planetary Science* 35: A158–159.

Treiman A. H. and Romanek C. S. 1998. Bulk and stable isotopic compositions of carbonate minerals in martian meteorite Allan Hills 84001: No proof of high formation temperature. *Meteoritics & Planetary Science* 33:737–742.

Treiman A. H., Amundsen H. E. F., Blake D. F., and Bunch T. E. 2002. Hydrothermal origin for carbonate globules in martian meteorite ALH 84001: A terrestrial analogue from Spitzbergen (Norway). *Earth and Planetary Science Letters* 204:323-332.

Tyburczy J. A. and Ahrens T. J. 1986. Dynamic compression and volatile release of carbonates. *Journal of Geophysical Research* 91:4730–4744.

Valley J. W., Eiler J. M., Graham C. M., Gibson E. K., Romanek C. S., and Stolper E. M. 1997. Low-temperature carbonate concretions in the martian meteorite ALH 84001: Evidence from stable isotopes and mineralogy. *Science* 275:1633–1638.

Vecht A. and Ireland T. G. 2000. The role of vaterite and aragonite in the formation of pseudo-biogenic carbonate structures: Implications for martian exobiology. *Geochimica et Cosmochimica Acta* 64:2719–2725.

Warren P. H. 1998. Petrologic evidence for low-temperature, possibly flood-evaporitic origin of carbonates in the ALH 84001 meteorite. *Journal of Geophysical Research* 103:16759–16773.

Warren P .H. 1999. Reply. *Journal of Geophysical Research* 104: 24217–24221.

Wenk H. R., Barber D. J., and Reeder R. J. 1983. Microstructures in carbonates. In *Carbonates: Mineralogy and chemistry,* edited by Reeder R. J. Washington D.C.: Mineralogical Society of America. pp. 301–367. *Reviews in Mineralogy* 11:301–367.

Weiss B. P., Kirschvink J. L., Baudenbacher F. J., Vali H., Peters N. T., MacDonald F. A., and Wikswo J. P. 2001. A low temperature transfer of ALH 84001 from Mars to Earth. *Science* 290:791–795.

Weiss B. P., Vali H., Baudenbacher F. J., Kirschvink J. L., Stewart S. T., and Shuster D. L. 2002. Records of an ancient martian magnetite field in ALH 84001. *Earth and Planetary Science Letters* 201:449–463.

Wilmot N., Barber D. J., Taylor J., and Graham A. L. 1992. Electron microscopy of molluscan crossed-lamellar microstructure. *Philosphical Transactions of the Royal Society of London B* 337: 21–35.

Yamaguchi A. and Sekine T. 2000. Monomineralic mobilization of plagioclase by shock: An experimental study. *Earth and Planetary Science Letters* 175:289–296.